Protonation Studies with the Alkylidyne–Tungsten Complex $[NEt_4][closo\text{-}1,2\text{-}Me_2\text{-}3\text{-}(\equiv CC_6H_4CH_2OMe\text{-}2)\text{-}3,3\text{-}(CO)_2\text{-}3,1,2\text{-}WC_2B_9H_9]$ in the Presence of Donor Molecules: Crystal Structures of $closo\text{-}1,2\text{-}Me_2\text{-}8,9\text{-}(CH_2C_6H_4CH_2\text{-}2)\text{-}3,3\text{-}(CO)_2\text{-}3,3\text{-}(PHPh_2)_2\text{-}3,1,2\text{-}WC_2B_9H_7$ and $[NEt_4][closo\text{-}1,8\text{-}Me_2\text{-}10,11\text{-}(CH_2C_6H_4CH_2\text{-}2)\text{-}2\text{-}I\text{-}2,2,2\text{-}(CO)_3\text{-}2,1,8\text{-}WC_2B_9H_7]$

John C. Jeffery and Sihai Li

School of Chemistry, The University of Bristol, Bristol BS8 1TS, United Kingdom

F. Gordon A. Stone*

Department of Chemistry, Baylor University, Waco, Texas 76798-7348

Received November 12, 1991

Treatment of CH_2Cl_2 solutions of $[NEt_4][closo\text{-}1,2\text{-}Me_2\text{-}3\text{-}(\equiv CC_6H_4CH_2OMe\text{-}2)\text{-}3,3\text{-}(CO)_2\text{-}3,1,2\text{-}WC_2B_9H_9]$ (**1d**) at −78 °C with $HBF_4\cdot Et_2O$ in the presence of CO or $PHPh_2$ affords the complexes $closo\text{-}1,2\text{-}Me_2\text{-}8,9\text{-}(CH_2C_6H_4CH_2\text{-}2)\text{-}3,3\text{-}(CO)_2\text{-}3,3\text{-}(L)_2\text{-}3,1,2\text{-}WC_2B_9H_7$ (**6**, L = CO or $PHPh_2$). The structure of the product **6b**, with L = $PHPh_2$, has been established by X-ray diffraction. Crystals are monoclinic, of space group $P2_1/n$, with a = 9.520 (2) Å, b = 19.870 (4) Å, c = 20.849 (4) Å, and V = 3843 (1) Å^3 for Z = 4. The tungsten is ligated by two CO and two $PHPh_2$ groups with a *transoid*-$W(CO)_2(PHPh_2)_2$ arrangement. The metal atom is also η^5-coordinated by the open pentagonal CCBBB face of the nido-icosahedral C_2B_9 fragment. The cage system has an exo-polyhedral $CH_2C_6H_4CH_2$-2 bridge linking two boron vertices. One methylene group is attached to the boron in the β-site with respect to the two carbons in the pentagonal face, while the other methylene group is bonded to a boron in the B_5 ring above the CCB*B*B site. Treatment of **1d** with $HBF_4\cdot Et_2O$ in the presence of PPh_3 affords $closo\text{-}1,2\text{-}Me_2\text{-}8\text{-}(CH_2C_6H_4CH_2OMe\text{-}2)\text{-}3,3,3\text{-}(CO)_3\text{-}3\text{-}(PPh_3)\text{-}3,1,2\text{-}WC_2B_9H_8$ (**7a**). In contrast, $Ph_2PCH_2PPh_2$ yields $closo\text{-}1,2\text{-}Me_2\text{-}8,9\text{-}(CH_2C_6H_4CH_2\text{-}2)\text{-}3,3\text{-}(CO)_2\text{-}3,3\text{-}(Ph_2PCH_2PPh_2)\text{-}3,1,2\text{-}WC_2B_9H_7$ (**8**). A compound structurally similar to the latter is obtained if PhC≡CPh is the substrate molecule present during protonation. Addition of aqueous HI to CH_2Cl_2 solutions of **1d** gives $[NEt_4][closo\text{-}1,8\text{-}Me_2\text{-}10,11\text{-}(CH_2C_6H_4CH_2\text{-}2)\text{-}2\text{-}I\text{-}2,2,2\text{-}(CO)_3\text{-}2,1,8\text{-}WC_2B_9H_7]$ (**11**), the structure of which has been established by X-ray diffraction. The salt forms triclinic crystals, space group $P\bar{1}$, with two structurally similar but crystallographically independent ion pairs in the asymmetric unit: a = 8.784 (2) Å, b = 12.639 (3) Å, c = 28.712 (7) Å, V = 3150 (1) Å^3 for Z = 4. In the carborane fragment the icosahedral core has a 2,1,8-WC_2B_9 configuration, and there is no connectivity between the two carbon vertices. The tungsten is coordinated by three CO groups and by an iodide ligand. It is also η^5-coordinated by a CB_4 pentagonal face of the cage. The latter has an exo-polyhedral bridging $CH_2C_6H_4CH_2$-2 group, the methylene fragments of which link boron atoms in the two CB_4 pentagonal layers; these borons occupy the same cage vertices as in **6b**. Treatment of the iodo compound with $TlBF_4$ in the presence of $Bu^tC{\equiv}CH$ gives a mixture of the mono- and bis(alkyne) complexes $closo\text{-}1,8\text{-}Me_2\text{-}10,11\text{-}(CH_2C_6H_4CH_2\text{-}2)\text{-}2\text{-}(\eta\text{-}Bu^tC_2H)\text{-}2,2\text{-}(CO)_2\text{-}2,1,8\text{-}WC_2B_9H_7$ (**12**) and $closo\text{-}1,8\text{-}Me_2\text{-}10,11\text{-}(CH_2C_6H_4CH_2\text{-}2)\text{-}2,2\text{-}(\eta\text{-}Bu^tC_2H)_2\text{-}2\text{-}(CO)\text{-}2,1,8\text{-}WC_2B_9H_7$ (**13**). The NMR data (^{1}H, ^{13}C{^{1}H}, ^{11}B{^{1}H}, and ^{31}P{^{1}H} for the new compounds are reported and discussed in relation to the structures.

Introduction

The anionic icosahedral complex $[closo\text{-}1,2\text{-}Me_2\text{-}3\text{-}(\equiv CR)\text{-}3,3\text{-}(CO)_2\text{-}3,1,2\text{-}WC_2B_9H_9]^-$ (R = alkyl or aryl), with their exo-polyhedral alkylidyne groups, are highly reactive, particularly when used as reagents for preparing compounds with bonds between tungsten and other transition elements.[1] Recently, interesting results have been obtained by protonating the anionic alkylidyne–tungsten complexes in the presence of donor molecules.[2]

Addition of $HBF_4\cdot Et_2O$ to CO-saturated solutions of the salts $[NEt_4][closo\text{-}1,2\text{-}Me_2\text{-}3\text{-}(\equiv CR)\text{-}3,3\text{-}(CO)_2\text{-}3,1,2\text{-}WC_2B_9H_9]$ (**1a–c**; Chart I) affords the neutral complexes $closo\text{-}1,2\text{-}Me_2\text{-}8\text{-}(CH_2R)\text{-}3,3,3,3,3\text{-}(CO)_4\text{-}3,1,2\text{-}WC_2B_9H_8$ (R = Me (**2a**), C_6H_4Me-4 (**2b**), C_6H_4OMe-2 (**2c**) Chart I).[2a,e] In these products a cage boron vertex carries an exo-polyhedral CH_2R substituent, derived from the alkylidyne ligands in the precursors. Moreover, the boron atom attached to the CH_2R group occupies the β-site with respect to the two carbons in the open pentagonal CCB*B*B face of the *nido*-7,8-C_2B_9 fragment η^5-coordinated to the W atom. In contrast to the results obtained with $HBF_4\cdot Et_2O$, treatment of CH_2Cl_2 solutions of **1a–c**, or their $[PPh_4]^+$ or $[N(PPh_3)_2]^+$ analogues, at −78 °C with aqueous HCl or HI yields the anionic complexes $[closo\text{-}1,8\text{-}Me_2\text{-}11\text{-}(CH_2R)\text{-}2\text{-}X\text{-}2,2,2\text{-}(CO)_3\text{-}2,1,8\text{-}WC_2B_9H_8]^-$ (**3**, X = Cl, I; Chart I).[2c–e] X-ray diffraction and NMR studies have established that in the products **3a–c** there is no connectivity between the cage CMe groups. Thus, the synthesis of these salts involves a polytopal rearrangement of the icosahedral structure from 3,1,2-WC_2B_9 in the precursors to 2,1,8-WC_2B_9 in the anionic complexes formed.[3] In

(1) Stone, F. G. A. *Adv. Organomet. Chem.* **1990**, *31*, 53.
(2) (a) Brew, S. A.; Devore, D. D.; Jenkins, P. D.; Pilotti, M. U.; Stone, F. G. A. *J. Chem. Soc., Dalton Trans.* **1992**, 393. (b) Brew, S. A.; Jenkins, P. D.; Jeffery, J. C.; Stone, F. G. A. *J. Chem. Soc., Dalton Trans.* **1992**, 401. (c) Brew, S. A.; Carr, N.; Jeffery, J. C.; Pilotti, M. U.; Stone, F. G. A. *J. Am. Chem. Soc.* **1992**, *114*, 2203. (d) Brew, S. A.; Stone, F. G. A. *J. Chem. Soc., Dalton Trans.* **1992**, 867. (e) Jeffery, J. C.; Li, S.; Sams, D. W. I.; Stone, F. G. A. *J. Chem. Soc., Dalton Trans.* **1992**, 877. (f) Brew, S. A.; Jeffery, J. C.; Mortimer, M. D.; Stone, F. G. A. *J. Chem. Soc., Dalton Trans.* **1992**, 1365.

0276-7333/92/2311-1902$03.00/0

Chart I

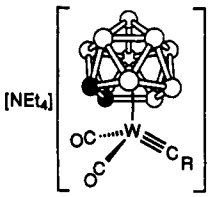

	R
1a	Me
1b	C_6H_4Me-4
1c	C_6H_4OMe-2
1d	$C_6H_4CH_2OMe$-2

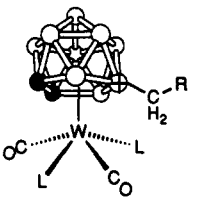

	R	L
2a	Me	CO
2b	C_6H_4Me-4	CO
2c	C_6H_4OMe-2	CO
2d	C_6H_4OMe-2	$PHPh_2$
2e	C_6H_4Me-4	$CNBu^t$

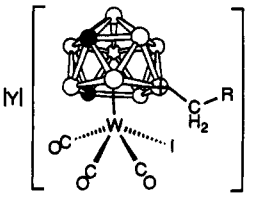

	Y	R
3a	NEt_4	Me
3b	PPh_4	C_6H_4Me-4
3c	NEt_4	C_6H_4OMe-2

● CMe ○ BH ⊕ B

Chart II

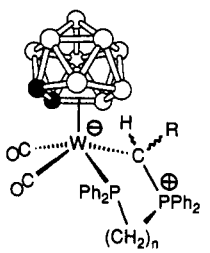

	R	n
4a	C_6H_4Me-4	1
4b	C_6H_4Me-4	2
4c	C_6H_4OMe-2	1

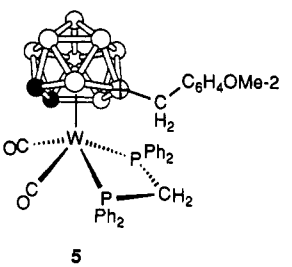

5

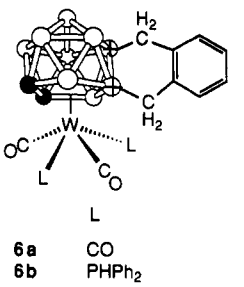

	L
6a	CO
6b	$PHPh_2$

● CMe ○ BH ⊕ B

compounds **3a–c** the CH_2R cage substituent is attached to the boron atom that was in the β-position relative to the carbon atoms in the CCB*B*B ring of the precursors. In this respect the species **3a–c** are similar to **2a–c**.

There is evidence[2] that the above syntheses proceed via the initial formation of alkylidene complexes *closo*-1,2-Me_2-3-(=C(H)R)-3,3-$(CO)_2$-3,1,2-$WC_2B_9H_9$, the electronically unsaturated W atoms of which would be expected to add CO or I^- readily. An associated insertion of the C(H)R groups into the β-BH fragment would then give the observed products, there being the additional requirement of a cage rearrangement process in order to yield **3a–c**. If the $[PPh_4]^+$ analogue of **1b** is treated with $HBF_4{\cdot}Et_2O$ in the presence of $Ph_2P(CH_2)_nPPh_2$ (n = 1, 2), the transient alkylidene complex is captured as the stable ylide compounds **4a,b**[2b] (Chart II). In contrast, if **1c** is protonated with $HBF_4{\cdot}Et_2O$ in the presence of $Ph_2PCH_2PPh_2$, the compound *closo*-1,2-Me_2-8-$(CH_2C_6H_4OMe$-2)-3,3-$(CO)_2$-3,3-$(Ph_2PCH_2PPh_2)$-3,1,2-$WC_2B_9H_8$ (**5**; Chart II) is obtained in ca. 80% yield, with the ylide complex **4c** formed only as a minor product.[2e]

These and other studies[2] reveal that the products obtained by protonating the salts **1a–c** depend both on the nature of the R group bonded to the alkylidyne carbon atom and on the acid used for protonation. In this paper[4] we describe protonation studies of the salt **1d**. It was anticipated that the $C_6H_4CH_2OMe$-2 substituent on the alkylidyne carbon atom would adopt a nonspectator role upon addition of $HBF_4{\cdot}Et_2O$ or HI to solutions of **1d** containing donor molecules.

Results and Discussion

Compound **1d**, required as a starting material for the experiments described herein, was obtained by treating $W(O_2CCF_3)(\equiv CC_6H_4CH_2OMe$-2)$(CO)_2(py)_2$ (py = pyridine) in tetrahydrofuran with $Na_2[7,8$-$C_2B_9H_9Me_2]$ in the same solvent, followed by addition of $[NEt_4]Cl$. The salt **1d** was fully characterized by the data listed in Tables I–III.

Treatment of CO-saturated solutions of **1d** at −78 °C with $HBF_4{\cdot}Et_2O$ afforded, after column chromatography of the reaction mixture on alumina, the complex *closo*-1,2-Me_2-8,9-$(CH_2C_6H_4CH_2$-2)-3,3,3,3-$(CO)_4$-3,1,2-$WC_2B_9H_7$ (**6a**; Chart II). It was impossible to establish fully the structure of this product solely on the basis of the NMR data, especially the arrangement of the cage substituents. Moreover, the complex decomposed during slow crystallization and so an X-ray diffraction study was not feasible. However, it was possible to obtain good-quality crystals of the related compound *closo*-1,2-Me_2-8,9-$(CH_2C_6H_4CH_2$-2)-3,3-$(CO)_2$-3,3-$(PHPh_2)_2$-3,1,2-$WC_2B_9H_7$ (**6b**) for an X-ray study.

Compound **6b** was obtained by treating CH_2Cl_2 solutions containing **1d** and 2 equiv of $PHPh_2$ with $HBF_4{\cdot}Et_2O$. Selected X-ray diffraction data are listed in Table IV, and

(3) The compounds **2a–c** may be regarded as containing [*nido*-7,8-$C_2B_9H_8$-10-(CH_2R)-7,8-$Me_2]^{2-}$ ligands, formally donating four electrons to a $W(CO)_4$ fragment. For convenience, and to emphasize the relationship with cyclopentadienylmetal chemistry, the ligand descriptor can be abbreviated to η^5-$C_2B_9H_8(CH_2R)Me_2$.[2a,d] However, in this paper, which describes compounds with both 3,1,2- and 2,1,8-WC_2B_9 core structures, we use the more cumbersome full atom labeling scheme for icosahedra so as to emphasize the different arrangements of the cage vertices. Hence, **3a** is $[NEt_4][closo$-1,8-Me_2-11-Et-2-I-2,2,2-$(CO)_3$-2,1,8-$WC_2B_9H_8]$.[2c]

(4) This paper is part 7 of a series on the chemistry of alkylidyne carborane complexes of the group 6 metals. For part 6 see ref 2f.

Table I. Analytical and Other Data for the Tungsten Compounds

compd no.	compd	color	yield/%	ν_{max}(CO)[a]/cm^{-1}	Anal.[b]/% C	Anal.[b]/% H
1d	[NEt_4][*closo*-1,2-Me_2-3-(≡$CC_6H_4CH_2OMe$-2)-3,3-$(CO)_2$-3,1,2-$WC_2B_9H_9$]	orange	89	1964 vs, 1880 vs	41.6 (41.6)[c]	7.2 (6.7)
6a	*closo*-1,2-Me_2-8,9-($CH_2C_6H_4CH_2$-2)-3,3,3,3-$(CO)_4$-3,1,2-$WC_2B_9H_7$	green	53	2092 vs, 2017 s, sh, 1999 vs, br	34.8 (34.4)	4.4 (3.8)
6b	*closo*-1,2-Me_2-8,9-($CH_2C_6H_4CH_2$-2)-3,3-$(CO)_2$-3,3-$(PHPh_2)_2$-3,1,2-$WC_2B_9H_7$[d]	yellow	68	1942 s, 1856 vs	51.6 (52.2)	5.5 (5.0)
7a	*closo*-1,2-Me_2-8-($CH_2C_6H_4CH_2OMe$-2)-3,3,3-$(CO)_3$-3-(PPh_3)-3,1,2-$WC_2B_9H_8$	yellow	61	2024 vs, 1951 s, 1924 vs	49.4 (49.5)	5.5 (4.9)
8	*closo*-1,2-Me_2-8,9-($CH_2C_6H_4CH_2$-2)-3,3-$(CO)_2$-3,3-$(Ph_2PCH_2PPh_2)$-3,1,2-$WC_2B_9H_7$	yellow	71	1965 vs, 1883 vs	52.8 (52.8)	5.3 (4.9)
9	*closo*-1,2-Me_2-8,9-($CH_2C_6H_4CH_2$-2)-3,3-(η-$PhC_2Ph)_2$-3-(CO)-3,1,2-$WC_2B_9H_7$	yellow	59	2070 vs	60.5 (59.3)	5.5 (5.0)
11	[NEt_4][*closo*-1,8-Me_2-10,11-($CH_2C_6H_4CH_2$-2)-2-I-2,2,2-$(CO)_3$-2,1,8-$WC_2B_9H_7$]	dark red	48	2008 vs, 1917 vs, br	35.5 (35.1)[e]	5.7 (5.3)
12	*closo*-1,8-Me_2-10,11-($CH_2C_6H_4CH_2$-2)-2-(η-Bu^tC_2H)-2,2-$(CO)_2$-2,1,8-$WC_2B_9H_7$	purple	9	2044 vs, 1980 vs	38.8 (39.3)[f]	6.0 (5.1)
13	*closo*-1,8-Me_2-10,11-($CH_2C_6H_4CH_2$-2)-2,2-(η-$Bu^tC_2H)_2$-2-(CO)-2,1,8-$WC_2B_9H_7$	pale yellow	39	2049 vs	46.7 (47.0)	6.6 (6.5)

[a] Measured in CH_2Cl_2. For all carborane compounds there is a broad B–H stretching absorption at 2550 cm^{-1}. [b] Calculated values are in parentheses. [c] N, 2.2 (2.1). [d] Mixture of isomers formed in ca. 2:1 ratio; see text. [e] N, 2.1 (1.8). [f] Crystallized with 0.5 molecule of CH_2Cl_2.

Table II. Hydrogen-1 and Carbon-13 NMR Data[a] for the Tungsten Compounds

compd no.	$\delta(^1H)$[b]	$\delta(^{13}C)$[c]
1d	1.19 (t, br, 12 H, CH_2*Me*, J_{HH} 7), 2.08 (s, 6 H, CMe), 3.04 (q, 8 H, C*H*$_2$Me, J_{HH} 7), 3.45 (s, 3 H, OMe), 4.83 (s, 2 H, CH_2), 7.16–7.48 (m, 4 H, C_6H_4)	295.9 (C≡W), 227.8 (CO, J_{WC} 182), 149.3, 138.5 [C^1, $C^2(C_6H_4)$], 129.5, 127.9, 127.8, 127.3 (C_6H_4), 72.3 (CH_2), 62.2 (*C*Me), 58.9 (OMe), 52.9 (*C*H$_2$Me), 29.9 (*CMe*), 7.7 (CH_2*Me*)
6a	2.02, 2.12 (AB, br, 2 H, BCH_2, J_{AB} 17), 2.23, 2.31 (AB, br, 2 H, BCH_2, J_{AB} 14), 2.41 (s, 3 H, CMe), 2.50 (s, 3 H, CMe), 6.94 (s, br, 4 H, C_6H_4)	209.6 (CO, J_{WC} 115), 142.6, 142.3 [C^1, $C^2(C_6H_4)$], 129.66, 129.65, 125.0, 124.7 (C_6H_4), 67.6, 66.5 (*C*Me), 33.1, 32.9 (*CMe*), 30.8, 26.3 (vbr, BCH_2)[d]
6b[e]	1.84* (d, 6 H, CMe, J_{PH} 2), 1.98 (s, br, 2 H, BCH_2), 2.10* (s, br, 2 H, BCH_2), 2.19* (s, br, 2 H, BCH_2), 2.31 (t, 3 H, CMe, J_{PC} 1), 2.33 (d, 3 H, CMe, J_{PH} 4), 2.23, 2.54 (AB, br, 2 H, BCH_2, J_{AB} 15), 6.08–7.92 (m, br, 26 H, C_6H_4, PH, Ph)	232.0 (t, CO, J_{PC} 24), 231.2 (t, CO, J_{PC} 31), 229.9* (AXX′, CO, *N*[f] 28), 145.0, 144.9*, 144.5, 144.3* [C^1, $C^2(C_6H_4)$], 135.4, 135.3, 134.6*, 134.5*, 124.8*, 124.6, 124.4 (C_6H_4), 134.0–129.0 (m, br, Ph), 64.5* (*C*Me), 60.0, 59.6 (*C*Me), 31.4* (*CMe*), 30.5 (vbr, BCH_2), 28.9, 28.6 (*CMe*), 25.9 (vbr, BCH_2)[d]
7a	1.82 (s, br, 2 H, BCH_2), 2.00 (s, 6 H, CMe), 3.34 (s, 3 H, OMe), 4.22 (s, 2 H, C*H*$_2$OMe), 6.68–7.13 (m, 4 H, C_6H_4), 7.52–7.72 (m, 15 H, Ph)	222.4 (d, 2 × CO, J_{PC} 29), 221.4 (d, CO, J_{PC} 9), 146.1, 135.8 [C^1, $C^2(C_6H_4)$], 134.2, 132.4 (Ph), 130.5 (C_6H_4), 129.3, 129.1 (Ph), 127.6, 126.4, 123.9 (C_6H_4), 73.4 (CH_2OMe), 67.1 (*C*Me), 58.5 (OMe), 31.4 (*CMe*), 27.8 (vbr, BCH_2)
8	1.27, 1.55 (AB, 2 H, BCH_2, J_{AB} 14), 1.84, 2.02 (AB, 2 H, BCH_2, J_{AB} 26), 2.24 (s, 6 H, CMe), 4.97 (d of t, 1 H, PCH_2P, J_{PH} 11, J_{HH} 15), 5.40 (d of t, 1 H, PCH_2P, J_{PH} 10, J_{HH} 15), 6.41–6.88 (m, 4 H, C_6H_4), 7.18–7.74 (m, 20 H, Ph)	233.6 (d of d, CO, J_{PC} 10 and 22), 232.6 (d of d, CO, J_{PC} 22 and 10), 144.1, 143.3 [C^1, $C^2(C_6H_4)$], 134.2, 133.4, 132.3 (Ph), 132.0, 131.9 (C_6H_4), 129.2 (Ph), 124.3, 124.0 (C_6H_4), 61.5, 59.8 (*C*Me), 50.8 (t, PCH_2P, J_{PC} 28), 34.0 (vbr, BCH_2), 32.7 (d, *CMe*, J_{PC} 7), 32.2 (*CMe*), 25.8 (vbr, BCH_2)
9[g,h]	1.39 (s, br, 3 H, CMe), 2.25 (s, br, 3 H, CMe), 1.93–2.52 (m, vbr, 4 H, BCH_2), 6.48–8.32 (m, 24 H, C_6H_4, Ph)	209.4 (CO), 189.3, 188.3, 175.9, 172.1 (C≡C), 145.3–123.8 (m, C_6H_4, Ph), 65.6, 62.0 (*C*Me), 30.0 (vbr, BCH_2), 29.2, 27.0 (*CMe*), 25.0 (vbr, BCH_2)
11	1.28 (t, br, 12 H, CH_2*Me*, J_{HH} 7), 1.55 (s, 3 H, CMe), 1.94 (s, 3 H, CMe), 2.02–2.44 (m, vbr, 4 H, BCH_2), 3.12 (q, 8 H, C*H*$_2$Me, J_{HH} 7), 6.87–6.97 (m, 4 H, C_6H_4)	230.8, 222.1, 221.3 (CO), 145.9, 142.9 [C^1, $C^2(C_6H_4)$], 129.8, 129.7, 124.5, 124.2 (C_6H_4), 61.4 (*C*Me), 61.1 (br, *C*Me), 54.0 (CH_2Me), 32.5 (*CMe*), 29.3 (*CMe*), 28.9, 24.8 (vbr, BCH_2), 8.0 (CH_2*Me*)
12[g]	1.13 (s, 3 H, CMe), 1.62 (s, 9 H, Bu^t), 1.90–2.38 (m, vbr, 4 H, BCH_2), 2.12 (s, 3 H, CMe), 6.60–7.00 (m, 4 H, C_6H_4), 10.88 (s, 1 H, CH)	217.5, 214.2 (CO), 208.9 (*C*Bu^t), 188.5 (CH), 142.6, 142.4 [C^1, $C^2(C_6H_4)$], 129.2, 129.0, 124.5 (C_6H_4), 65.3 (*C*Me), 65.0 (br, *C*Me), 41.6 (*C*Me$_3$), 32.0 (*CMe*), 30.9 (*CMe*$_3$), 30.4 (vbr, BCH_2), 28.6 (*CMe*), 25.3 (vbr, BCH_2)
13[e]	1.04 (s, 3 H, CMe), 1.15 (s, 9 H, Bu^t), 1.20–2.20 (m, vbr, 4 H, BCH_2), 1.41 (s, 9 H, Bu^t), 1.42* (s, 9 H, Bu^t), 1.50* (s, 9 H, Bu^t), 1.85* (s, 3 H, CMe), 2.11* (s, 3 H, CMe), 2.69 (s, 3 H, CMe), 6.60–6.90 (m, 4 H, C_6H_4), 9.38 (s, br, 1 H, CH), 10.18* (s, 1 H, CH), 10.37* (s, 1 H, CH), 10.48 (s, br, 1 H, CH)	216.4*, 216.3 (CO), 166.9, 165.5*, 165.4, 163.6* (≡CH), 154.0, 152.5 (br, ≡*C*Bu^t) 143.1*, 142.9, 142.3, 141.9*, 129.5, 129.4, 129.0*, 128.9*, 124.3, 124.2*, 123.9, 123.8* (C_6H_4), 67.8, 63.9*, 63.8* br, 61.1 br (*C*Me), 38.7, 38.4 (*C*Me$_3$), 30.9 (*CMe*), 30.8, 30.7 (*CMe*$_3$), 30.5 (vbr, BCH_2), 29.5 (*CMe*), 24.8 (vbr, BCH_2)

[a] Chemical shifts (δ) in ppm, coupling constants (J) in Hz. [b] Measured at ambient temperature in CD_2Cl_2 unless otherwise stated. Proton resonances for terminal B–H groups occur as broad unresolved peaks in the range δ ca. −2 to +3. [c] Hydrogen-1 decoupled, measured at ambient temperature in CD_2Cl_2 unless otherwise stated. Chemical shifts are positive to high frequency of $SiMe_4$. [d] Measured in CD_2Cl_2–CH_2Cl_2. [e] Peaks due to the minor isomer are listed with an asterisk. However, some resonances are obscured by those due to the major isomer. [f] $N = |J_{PC} + J_{PC'}|$. [g] Measured in $CDCl_3$. [h] Measured at −60 °C.

the molecule is shown in Figure 1. It is immediately apparent that the complex has a novel structure with the cage boron atoms B(4) and B(9) bridged by a $CH_2C_6H_4C$-H_2-2 fragment. The atom B(4) lies in the open pentagonal C_2B_3 face of the *nido*-C_2B_9 cage η^5-coordinated to the W atom and is in the β-site with respect to the carbons. The atom B(9) lies above B(4) in the B_5 pentagonal ring. The metal atom is ligated by two CO molecules, in an essentially linear manner, and by two $PHPh_2$ groups, which adopt a transoid arrangement (P(1)–W–P(2) = 129.7 (1)°).

Evidently in the formation of **6b** the OMe group in the precursor **1d** has been lost, presumably as MeOH. The

Table III. Boron-11 and Phosphorus-31 NMR[a] Data for the New Tungsten Compounds

compd no.	$\delta(^{11}B)$[b]	$\delta(^{31}P)$[c]
1d[d]	−8.2 (2 B, BH), −11.5 (2 B, BH), −12.1 (2 B, BH), −14.9 (2 B, BH), −17.0 (1 B, BH)	
6a	9.1 (1 B, BCH_2), 7.7 (1 B, BCH_2), 0.5 (1 B, BH), −0.3 (1 B, BH), −7.1 (2 B, BH), −7.6 (1 B, BH), −8.5 (2 B, BH)	
6b[d]	7.7 (1 B, BCH_2), 4.2 (1 B, BCH_2), −2.7 (1 B, BH), −4.7 (1 B, BH), −6.4 (1 B, BH), −7.6 (1 B, BH), −8.7 (1 B, BH), −10.9 (2 B, BH)	18.0* (s, J_{WP} 194), 15.3, 15.1 (AB, J_{AB} 29, J_{WP} 193 and 183)[e]
7a	6.8 (1 B, BCH_2), −3.9 (1 B, BH), −5.4 (2 B, BH), −8.8 (3 B, BH), −10.0 (2 B, BH)	10.0 (s, J_{WP} 163)
8	7.1 (1 B, BCH_2), 3.7 (1 B, BCH_2), −3.1 (2 B, BH), −6.5 (2 B, BH), −8.7 (2 B, BH), −11.9 (1 B, BH)	−32.2, −32.5 (AB, J_{AB} 56, J_{WP} 168 and 214)
9[f]	11.1 (1 B, BCH_2), 5.6 (1 B, BCH_2), −1.4 to −9.7 (br, 7 B, BH)	
11[d]	3.9 (1 B, BCH_2), −0.3 (1 B, BCH_2), −2.4 (2 B, BH), −8.3 (1 B, BH), −11.3 (1 B, BH), −13.5 (1 B, BH), −15.6 (1 B, BH), −20.5 (1 B, BH)	
12[f]	8.2 (1 B, BCH_2), 4.1 (1 B, BCH_2). −0.4 to −12.3 (7 B, BH)	
13[d,g]	9.1 (1 B, BCH_2), 7.8* (1 B, BCH_2), 5.1* (1 B, BCH_2), 3.6 (1 B, BCH_2), −0.4 to −13.6 (14 BH for both isomers)	

[a] Chemical shifts (δ) in ppm, coupling constants (J) in Hz. [b] Hydrogen-1 decoupled, measured at ambient temperature in CD_2Cl_2 unless otherwise stated. Chemical shifts are positive to high frequency of $BF_3{\cdot}Et_2O$ (external). Signals ascribed to more than one boron nucleus may result from overlapping peaks and do not necessarily indicate symmetry equivalence. [c] Hydrogen-1 decoupled, measured at ambient temperature in CD_2Cl_2. Chemical shifts are positive to high frequency of 85% H_3PO_4 (external). [d] Measured in CD_2Cl_2–CH_2Cl_2. [e] Mixture of transoid and cisoid isomers (see text), peak intensities indicating a 2:1 isomer ratio. Signals due to cisoid species are marked with an asterisk. [f] Measured in $CDCl_3$. [g] Peaks due to the minor isomer are marked with an asterisk.

Table IV. Selected Bond Lengths (Å) and Angles (deg) for *closo*-1,2-Me_2-8,9-($CH_2C_6H_4CH_2$-2)-3,3-$(CO)_2$-3,3-$(PHPh_2)_2$-3,1,2-$WC_2B_9H_7$ (6b)

W–P(1)	2.470 (2)	W–P(2)	2.489 (2)	W–C(1)	2.453 (6)	W–C(2)	2.446 (6)
W–B(3)	2.375 (7)	W–B(4)	2.419 (6)	W–B(5)	2.363 (6)	W–C(20)	1.982 (6)
W–C(21)	1.971 (6)	P(1)–H(1)	1.35 (8)	P(1)–C(41)	1.852 (6)	P(1)–C(51)	1.826 (7)
P(2)–H(2)	1.46 (7)	P(2)–C(61)	1.835 (5)	P(2)–C(71)	1.821 (6)	C(1)–C(2)	1.620 (8)
C(1)–C(3)	1.532 (9)	C(2)–C(4)	1.532 (9)	B(4)–B(9)	1.772 (9)	B(4)–C(30)	1.63 (1)
B(9)–C(37)	1.60 (1)	C(20)–O(20)	1.148 (8)	C(21)–O(21)	1.154 (7)	C(30)–C(31)	1.498 (9)
C(31)–C(36)	1.406 (8)	C(36)–C(37)	1.52 (1)				

P(1)–W–P(2)	129.7 (1)	P(1)–W–C(20)	77.7 (2)	P(2)–W–C(20)	79.7 (2)
P(1)–W–C(21)	72.6 (2)	P(2)–W–C(21)	71.6 (2)	C(20)–W–C(21)	106.1 (3)
W–P(1)–H(1)	116 (3)	W–P(1)–C(41)	120.4 (2)	H(1)–P(1)–C(41)	104 (3)
W–P(1)–C(51)	118.8 (2)	H(1)–P(1)–C(51)	90 (3)	C(41)–P(1)–C(51)	103.0 (3)
W–P(2)–H(2)	107 (3)	W–P(2)–C(61)	123.5 (2)	H(2)–P(2)–C(61)	102 (3)
W–P(2)–C(71)	118.0 (2)	C(61)–P(2)–C(71)	101.9 (3)	W–C(1)–C(3)	109.6 (4)
C(2)–C(1)–C(3)	121.1 (5)	C(2)–C(1)–B(5)	109.9 (4)	W–C(2)–C(4)	110.7 (4)
C(1)–C(2)–C(4)	120.5 (5)	C(1)–C(2)–B(3)	110.4 (5)	C(4)–C(2)–B(3)	125.0 (4)
C(2)–B(3)–B(4)	107.7 (4)	B(3)–B(4)–B(5)	102.3 (5)	B(9)–B(4)–C(30)	107.4 (5)
C(1)–B(5)–B(4)	109.5 (5)	B(4)–B(9)–C(37)	112.8 (5)	W–C(20)–O(20)	175.7 (6)
W–C(21)–O(21)	176.2 (6)	B(4)–C(30)–C(31)	110.4 (5)	C(30)–C(31)–C(32)	121.8 (5)
C(30)–C(31)–C(36)	119.3 (6)	C(32)–C(31)–C(36)	118.9 (6)	C(31)–C(32)–C(33)	120.8 (6)
C(32)–C(33)–C(34)	120.2 (7)	C(33)–C(34)–C(35)	119.9 (7)	C(34)–C(35)–C(36)	121.0 (6)
C(31)–C(36)–C(35)	119.2 (6)	C(31)–C(36)–C(37)	119.6 (5)	C(35)–C(36)–C(37)	121.1 (5)
B(9)–C(37)–C(36)	111.4 (5)	P(1)–C(41)–C(42)	118.7 (5)		

unusual and unexpected structure of **6b** contrasts with that of *closo*-1,2-Me_2-8-($CH_2C_6H_4OMe$-2)-3,3-$(CO)_2$-3,3-$(PHPh_2)_2$-3,1,2-$WC_2B_9H_8$ (**2d**), prepared by adding $HBF_4{\cdot}Et_2O$ to a CH_2Cl_2 solution of **1c** containing 2 equiv of $PHPh_2$.[2e]

Having established the structure of **6b**, it is possible to interpret the spectroscopic data for this compound. Moreover, complex **6a** must have a similar structure, since the ^1H, $^{13}C\{^1H\}$, and $^{11}B\{^1H\}$ NMR spectra show features similar to those of **6b**. However, examination of the NMR spectra of the latter revealed that it is formed as a mixture of two isomers, since the resonances for the various groups appeared in duplicate. On the basis of relative peak intensities in the $^{31}P\{^1H\}$ spectrum, the isomers of **6b** are present in solutions in a ca. 2:1 ratio. Similar behavior has been observed previously for compound **2e**, obtained from **1b**, $CNBu^t$, and $HBF_4{\cdot}Et_2O$.[2a] The isomerism of **6b** and **2e** may be attributed to transoid and cisoid arrangements of the $W(CO)_2L_2$ (L = $PHPh_2$ or $CNBu^t$) groups in these molecules. Only the transoid isomer of **6b** is shown in the structural formula. It is evident from the $^{31}P\{^1H\}$ NMR spectrum (Table III) that the major isomer has the *transoid*-$W(CO)_2(PHPh_2)_2$ arrangement, as found in the crystal. The more intense peaks of the major isomer display an AB pattern: δ 15.1 and 15.3, with J_{AB} = 29 Hz and J_{WP} = 183 and 193 Hz.

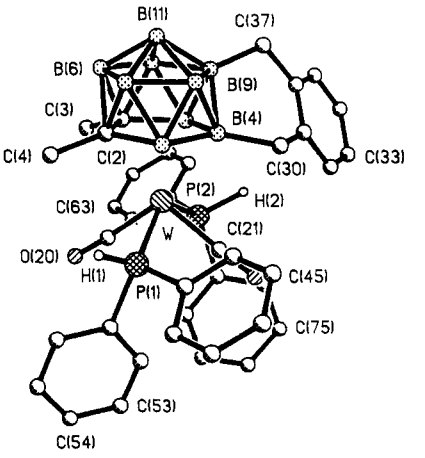

Figure 1. Structure of *closo*-1,2-Me_2-8,9-($CH_2C_6H_4CH_2$-2)-3,3-$(CO)_2$-3,3-$(PHPh_2)_2$-3,1,2-$WC_2B_9H_7$ (**6b**), showing the crystallographic atom-labeling scheme.

The presence of the BCH_2 groups in **6a,b** is clearly revealed in the $^{11}B\{^1H\}$ NMR spectra (Table III), with di-

Chart III

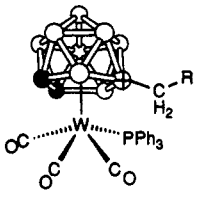

R

7a $C_6H_4CH_2OMe$-2
7b C_6H_4Me-4
7c C_6H_4OMe-2

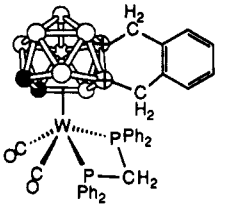

8

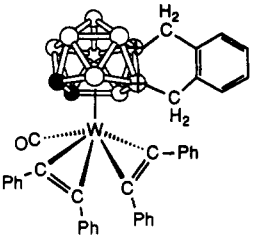

9

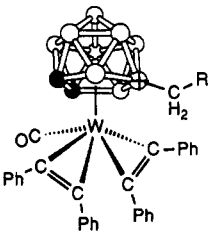

R

10a C_6H_4Me-4
10b C_6H_4OMe-2

● CMe ○ BH ⊕ B

agnostic peaks at δ 9.1 and 7.7 (**6a**) and δ 7.7 and 4.2 (**6b**). The BCH_2 resonances for **2c,d** occur in the same region at δ 8.6 and 7.4, respectively.[2e] Signals for the BCH_2 groups in the $^{13}C\{^1H\}$ NMR spectra are seen as broad peaks at δ 30.8 and 26.3 for **6a** and at 30.5 and 25.9 for **6b** (major isomer). These chemical shifts may be compared with those found for the BCH_2 groups of **2c,d** at δ 28.3 and 25.0, respectively.[2e] Resonances for the nonequivalent BCH_2 groups are also observed in the ^1H NMR spectra of **6a,b**. Thus, the spectrum of the former species is sufficiently well resolved for the signals to appear as two distinct AB patterns at δ 2.02 and 2.12 (J_{AB} = 17 Hz) and at δ 2.23 and 2.31 (J_{AB} = 14 Hz).

The protonation of **1d** with $HBF_4{\cdot}Et_2O$ in the presence of PPh_3 was next investigated and found to give *closo*-1,2-Me_2-8-($CH_2C_6H_4CH_2OMe$-2)-3,3,3-$(CO)_3$-3-(PPh_3)-3,1,2-$WC_2B_9H_8$ (**7a**; Chart III). This product was fully characterized by the data given in Tables I–III. It is structurally similar to the complexes **7b,c** obtained previously in similar reactions using the salts **1b,c** as precursors.[2a,e] The nature of compound **7a**, which has retained its $C_6H_4CH_2OMe$-2 group, is surprising in view of the structures of **6a,b**. It is noteworthy, however, that if **1d** is treated with $HBF_4{\cdot}Et_2O$ at −78 °C, and PPh_3 is subsequently added to the mixture at the same temperature, the only product is the tetracarbonyl species **6a**. This suggests that if $HBF_4{\cdot}Et_2O$ is added to **1d** in the presence of PPh_3, compound **7a** is formed in an early reaction step. The bulky PPh_3 ligand at the tungsten center might then reduce the flexibility of the $CH_2C_6H_4CH_2OMe$-2 group so that the OMe substituent is unable to approach the B(9)H vertex as a prelude to loss of MeOH by a process as yet unclear. It is noteworthy that the X-ray diffraction study of compound **7c** revealed appreciable steric interaction between the $CH_2C_6H_4OMe$-2 group and one of the Ph rings of the PPh_3 ligand.[2e] Similar constraints in **7a** might force the $CH_2C_6H_4CH_2OMe$-2 substituent away from the cage, inhibiting further reaction.

Treatment of CH_2Cl_2 solutions containing **1d** and $Ph_2PCH_2PPh_2$ at −78 °C with $HBF_4{\cdot}Et_2O$ affords *closo*-1,2-Me_2-8,9-($CH_2C_6H_4CH_2$-2)-3,3-$(CO)_2$-3,3-$(Ph_2PCH_2PPh_2)$-3,1,2-$WC_2B_9H_7$ (**8**; Chart III). The IR spectrum shows two CO absorptions at 1965 and 1883 cm^{-1}, similar to those observed[2e] in compound **5** at 1959 and 1874 cm^{-1}. In the $^{31}P\{^1H\}$ NMR spectrum of **8** there is a typical AB spin pattern: δ −32.2 and −32.5 with J_{AB} = 56 Hz and ^{183}W satellite peaks (J_{WP} = 168 and 214 Hz). The $^{11}B\{^1H\}$ NMR spectrum shows resonances at δ 7.1 and 3.7 for the BCH_2 nuclei. In the spectrum of **5** the signal for the single BCH_2 peak is at δ 7.0. This suggests that the peak at δ 7.1 in the spectrum of **8** is due to the BCH_2 moiety in the pentagonal open face of the *nido*-C_2B_9 cage ligating the tungsten atom.

In the ^1H NMR spectrum there are two AB spin patterns, one at δ 1.27 and 1.55 with J_{AB} = 14 Hz and the other at δ 1.84 and 2.02 with J_{AB} = 16 Hz, which are assigned to the two BCH_2 groups. The $^{13}C\{^1H\}$ NMR spectrum displays two resonances for the two nonequivalent CO ligands (Table II). Signals in this spectrum at δ 61.5 and 59.8 can be assigned to the cage *C*Me vertices. Peaks for the two nonequivalent C*Me* groups are also observed at δ 32.7 and 32.2. As expected, there are two very broad resonances centered at δ 34.0 and 25.8 due to the two BCH_2 groups. The C_6H_4 moiety gives rise to six resonances, occurring in three pairs (δ): 144.1, 143.3; 132.0, 131.9; 124.3, 124.0. The data indicate that although the aryl C_6H_4 groups have six nonequivalent carbon nuclei, there are three pairs of pseudoequivalent carbons, in agreement with the molecular structures. In the synthesis of **8** there was no evidence for the formation of an ylide complex akin to the complexes **4**.

Addition of $HBF_4{\cdot}Et_2O$ to a CH_2Cl_2 solution containing **1d** and 2 equiv of PhC≡CPh at −78 °C gives *closo*-1,2-Me_2-8,9-($CH_2C_6H_4CH_2$-2)-3,3-(η-$PhC_2Ph)_2$-3-(CO)-3,1,2-$WC_2B_9H_7$ (**9**; Chart III). This product is related to the compounds **10**, prepared similarly from the reagents **1b,c**.[2a,e] The IR spectrum of **9** shows one CO band (2070 cm^{-1}), as expected. Resonances in the ^1H and $^{13}C\{^1H\}$ NMR spectra measured at room temperature were too broad to be interpreted, due to the dynamic behavior of the molecule. This feature is related to rotation of the alkyne ligands.[2a,e] However, from spectra measured at −60 °C assignment of resonances is possible. In the ^1H NMR spectrum signals for nonequivalent CMe groups are observed at δ 1.39 and 2.25, but only one very broad multiplet (δ 1.93–2.52) is seen for the BCH_2 fragments. In the $^{13}C\{^1H\}$ NMR spectrum the nonequivalent cage CMe groups give signals at δ 65.6 and 62.0 (*C*Me) and 29.2 and 27.0 (C*Me*). There are, as expected, two very broad BCH_2 resonances

Table V. Selected Bond Lengths (Å) and Angles (deg) for [NEt_4][*closo*-1,8-Me_2-10,11-($CH_2C_6H_4CH_2$-2)-2-I-2,2,2-$(CO)_3$-2,1,8-$WC_2B_9H_7$] (11) (One of Two Independent Anions)

W(1)-I(1)	2.894 (2)	W(1)-C(121)	1.93 (2)	W(1)-C(122)	1.98 (2)	W(1)-C(123)	1.97 (3)
W(1)-C(101)	2.44 (2)	W(1)-B(102)	2.34 (2)	W(1)-B(103)	2.32 (2)	W(1)-B(104)	2.39 (2)
W(1)-B(105)	2.39 (2)	C(121)-O(121)	1.20 (3)	C(122)-O(122)	1.11 (3)	C(123)-O(123)	1.23 (3)
C(101)-C(102)	1.51 (3)	C(101)-B(102)	1.74 (3)	C(101)-B(105)	1.70 (3)	B(102)-B(103)	1.82 (3)
B(102)-C(107)	1.73 (3)	B(104)-B(105)	1.83 (3)	B(104)-B(109)	1.78 (3)	B(104)-C(130)	1.63 (3)
B(106)-C(107)	1.71 (4)	C(107)-C(108)	1.55 (3)	C(107)-B(108)	1.71 (3)	C(107)-B(111)	1.69 (3)
B(109)-B(110)	1.78 (3)	B(109)-B(111)	1.81 (3)	B(109)-C(137)	1.55 (3)	C(130)-C(131)	1.53 (2)
C(131)-C(136)	1.39 (3)	C(132)-C(133)	1.38 (3)	C(136)-C(137)	1.49 (3)		

I(1)-W(1)-C(121)	73.3 (6)	I(1)-W(1)-C(122)	129.4 (7)	C(121)-W(1)-C(122)	75.1 (9)
I(1)-W(1)-C(123)	71.9 (7)	C(121)-W(1)-C(123)	104.6 (8)	C(122)-W(1)-C(123)	79 (1)
W(1)-C(121)-O(121)	173 (2)	W(1)-C(122)-O(122)	176 (2)	W(1)-C(123)-O(123)	168 (2)
C(102)-C(101)-B(102)	121 (2)	C(102)-C(101)-B(105)	124 (2)	B(102)-C(101)-B(105)	109 (1)
C(101)-B(102)-B(103)	110 (1)	B(103)-B(104)-C(130)	128 (2)	B(105)-B(104)-C(130)	124 (2)
B(109)-B(104)-C(130)	107 (1)	C(101)-B(105)-B(104)	110 (2)	B(102)-C(107)-C(108)	113 (2)
B(103)-C(107)-C(108)	113 (2)	B(106)-C(107)-C(108)	118 (2)	B(102)-C(107)-B(108)	114 (2)
B(103)-C(107)-B(108)	62 (1)	B(106)-C(107)-B(108)	117 (2)	C(108)-C(107)-B(108)	119 (2)
C(108)-C(107)-B(111)	121 (2)	B(108)-C(107)-B(111)	64.7 (1)	B(104)-B(109)-C(137)	115 (2)
B(104)-C(130)-C(131)	115 (2)	C(130)-C(131)-C(132)	123 (2)	C(130)-C(131)-C(136)	120 (2)
C(131)-C(136)-C(137)	121 (2)	C(135)-C(136)-C(137)	121 (2)	B(109)-C(137)-C(136)	112 (2)

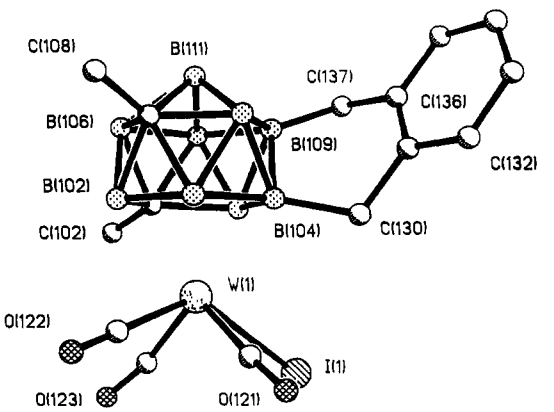

Figure 2. Structure of the anion of [NEt_4][*closo*-1,8-Me_2-10,11-($CH_2C_6H_4CH_2$-2)-2-I-2,2,2-$(CO)_3$-2,1,8-$WC_2B_9H_7$] (11), showing the crystallographic atom-labeling scheme.

at δ 30.0 and 25.0. Correspondingly, in the $^{11}B\{^1H\}$ NMR spectrum the BCH_2 moieties give diagnostic peaks at δ 11.1 and 5.6.

The chemical shifts of the ligated carbon atoms of the PhC≡CPh groups in the $^{13}C\{^1H\}$ NMR spectrum of **9** are of interest. The resonances are observed at δ 189.3, 188.3, 175.9, and 172.1, and the existence of four peaks corresponds to a limiting low-temperature spectrum with no rotation of the alkynes. The chemical shifts are in the region expected for alkynes donating three electrons to a metal atom.[5] This would enable the tungsten (d^6) to attain a filled 18-electron shell in complex **9** with 2 electrons from the CO ligand, 4 electrons from the *nido*-η^5-C_2B_9 cage, and 6 electrons from the two alkyne molecules.

As mentioned in the Introduction, compounds **1a–c** with HI afford the complexes **3**, in which the carbon atom vertices are no longer connected.[2c,e] Solutions of **1d** in CH_2Cl_2 with HI give the salt [NEt_4][*closo*-1,8-Me_2-10,11-($CH_2C_6H_4CH_2$-2)-2-I-2,2,2-$(CO)_3$-2,1,8-$WC_2B_9H_7$] (11; Chart IV), the structure of which was fully established by X-ray diffraction. The data revealed that **11** crystallized with two structurally similar but crystallographically independent ion pairs in the asymmetric unit. Selected structural parameters for one anion are given in Table V, and the anion is shown in Figure 2. It is immediately apparent that the cage has the 2,1,8-WC_2B_9 arrangement, as found in the compounds **3** and other species derived

Chart IV

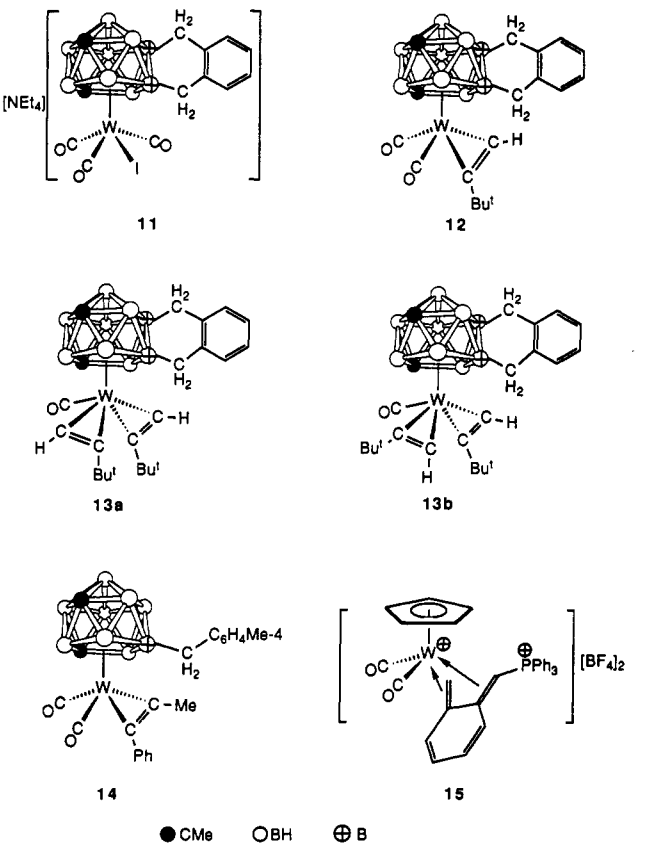

from the latter.[2c,6] As in compound **6b**, the *nido*-C_2B_9 fragment in **11** has an exo-polyhedral $CH_2C_6H_4CH_2$-2 bridge system linking two boron atoms (B(104) and B(109)). Moreover, the polytopal cage rearrangement has not influenced the relative sites of the BCH_2 linkages, which are the same as in **6b**. The B–CH_2–C_6H_4 bond angles (112 (2) and 115 (2)°) are comparable with those in **6b** (110.4 (5) and 111.4 (5)°). The tungsten atom, in addition to being ligated by the C_2B_9 fragment in the usual η^5-bonding mode, is coordinated by the iodide ligand and by three CO molecules, one of which deviates somewhat from linearity (W(1)–C(123)–O(123) = 168 (2)°). The structural parameters for **11** and **6b** are similar, apart from

(5) Templeton, J. L. *Adv. Organomet. Chem.* **1989**, *29*, 1 and references therein.

(6) Brew, S. A.; Jeffery, J. C.; Pilotti, M. U.; Stone, F. G. A. *J. Am. Chem. Soc.* **1990**, *112*, 6149.

differences produced by the different sites of the cage carbons.

The NMR data for **11** are in agreement with the structure established by X-ray diffraction. In the $^{13}C\{^1H\}$ NMR spectrum the resonances for the cage *C*Me vertices are at δ 61.4 and 61.1. The latter peak is appreciably broader than the former and may therefore be assigned to C(107) (Figure 2) for reasons discussed previously.[2c] The nonequivalent C*Me* groups give peaks at δ 32.5 and 29.3, and those for the BCH_2 groups are at δ 28.9 and 24.8. The pseudosymmetrical C_6H_4 fragment is revealed by three pairs of resonances (δ): 145.9, 142.9; 129.8, 129.7; 124.5, 124.2. As expected, there are three CO peaks, and these occur at δ 230.8, 222.1, and 221.3.

Treatment of CH_2Cl_2 solutions of **11** with $Bu^tC{\equiv}CH$ in the presence of $TlBF_4$ afforded a mixture of the species *closo*-1,8-Me_2-10,11-$(CH_2C_6H_4CH_2$-2)-2-(η-Bu^tC_2H)-2,2-$(CO)_2$-2,1,8-$WC_2B_9H_7$ (**12**) and *closo*-1,8-Me_2-10,11-$(CH_2C_6H_4CH_2$-2)-2,2-(η-$Bu^tC_2H)_2$-2-(CO)-2,1,8-$WC_2B_9H_7$ (**13**) (Chart IV). Examination of the ^1H, $^{13}C\{^1H\}$ (Table II), and $^{11}B\{^1H\}$ (Table III) NMR data for **12** and **13** establish that these products contain the $CH_2C_6H_4CH_2$-2 exo-polyhedral cage bridge system found in their precursor **11**. The pattern observed for the resonances of the *C*Me nuclei in the $^{13}C\{^1H\}$ NMR spectrum of **12** with one peak sharp (δ 65.3) and the other broad (δ 65.0) is in accord with the 2,1,8-WC_2B_9 icosahedral arrangement. However, duplication of peaks in the ^1H and $^{13}C\{^1H\}$ spectra of **13** showed that this bis(alkyne) complex was formed as a mixture of the two isomers **13a,b**. On the basis of the relative intensities of the signals the isomer ratio is ca. 2:1. However, assignment of signals to a particular isomer was not possible.

Compound **12** is closely related to the compound *closo*-1,8-Me_2-11-$(CH_2C_6H_4Me$-4)-2-(η-MeC_2Ph)-2,2-$(CO)_2$-2,1,8-$WC_2B_9H_8$ (**14**; Chart IV), obtained by treating **3b** with $AgBF_4$ in the presence of $MeC{\equiv}CPh$. The structure of **14** has been established by X-ray diffraction.[2c] In the $^{13}C\{^1H\}$ NMR spectrum of **12** the resonances for the ligated carbons of the alkyne occur at δ 208.9 and 188.5, in the chemical shift range associated empirically with the alkyne donating four electrons to the metal center.[5]

Conclusions

The new compounds described in this paper further illustrate the diverse nature of the species obtainable by protonating the salts **1**. As far as we are aware, those products containing exo-polyhedral cage $CH_2C_6H_4CH_2$-2 groups are structurally without precedent. Their mode of formation is at present obscure. However, a similar loss of an OMe fragment from a precursor containing a $W{\equiv}CC_6H_4CH_2OMe$-2 group has recently been observed by us.[7] Treatment of a mixture of $[W(\equiv CC_6H_4CH_2OMe$-2)$(CO)_2(\eta^5$-$C_5H_5)]$ and PPh_3 in CH_2Cl_2 at −78 °C with $HBF_4{\cdot}Et_2O$ affords the complex $[W(CO)_2\{\eta^4$-$C_6H_4(CH_2)$-$[CH(PPh_3)]$-1,2$\}(\eta^5$-$C_5H_5)][BF_4]_2$ (**15**; Chart IV). The work reported herein has also further demonstrated the novel cage framework rearrangement observed when aqueous HI is used instead of $HBF_4{\cdot}Et_2O$ for protonation of salts of type **1**.

Experimental Section

General Considerations. All reactions were conducted under an atmosphere of dry nitrogen using Schlenk-line techniques. Solvents were distilled from appropriate drying agents under nitrogen before use. Chromatography columns (ca. 15 cm in length and 2 cm in diameter unless otherwise stated) were packed with aluminia (Brockman Activity III). Spectroscopic measurements were made using instrumentation described previously.[2] The $HBF_4{\cdot}Et_2O$ used for protonation was purchased from Aldrich (85% $HBF_4{\cdot}Et_2O$ in Et_2O). Analytical and other data for the new compounds are given in Table I.

Table VI. Crystallographic Data for 6b and 11[a]

	6b	11
cryst dimens, mm	0.30 × 0.50 × 0.20	0.40 × 0.45 × 0.30
formula	$C_{38}H_{43}B_9O_2P_2W$	$C_{23}H_{41}B_9INO_3W$
M_r	874.8	787.6
cryst color, shape	yellow prisms	orange cubes
cryst syst	monoclinic	triclinic
space group	$P2_1/n$	$P\bar{1}$
a, Å	9.520 (2)	8.784 (2)
b, Å	19.870 (4)	12.639 (3)
c, Å	20.849 (4)	28.712 (7)
α, deg	90.00	89.40 (2)
β, deg	102.95 (2)	81.17 (2)
γ, deg	90.00	89.38 (2)
V, Å^3	3843 (1)	3150 (1)
Z	4	4
d_{calcd}, g cm^{-3}	1.68	1.66
μ(Mo Kα), cm^{-1}	31.8	47.4
F(000), e	1744	1528
T, K	293	293
no. of unique reflns	7473	11 922
no. of obsd rflns	4923	6551
criterion for obsd n [$F_o \geq n\sigma(F_o)$]	5	5
R (R')[b]	0.031 (0.031)	0.068 (0.067)
final electron density diff features (max/min), e Å^{-3}	+1.34/−0.82	+2.13/−2.30

[a] Data collected on a Siemens R3m/V four-circle diffractometer operating in the Wyckoff ω-scan mode in the range $5° \leq 2\theta \leq 50°$; graphite-monochromated Mo Kα X-radiation, $\bar{\lambda}$ = 0.710 69 Å. Refinement was by full-matrix least squares with a weighting scheme of the form $w^{-1} = [\sigma^2(F_o) + g|F_o|^2]$ with g = 0.0004 (**6b**), 0.0005 (**11**); $\sigma^2(F_o)$ is the variance in F_o due to counting statistics. g was chosen so as to minimize variation in $\sum w(|F_o| - |F_c|)^2$ with $|F_o|$. [b] $R = \sum||F_o| - |F_c||/\sum|F_o|$, $R' = \sum w^{1/2}||F_o| - |F_c||/\sum w^{1/2}|F_o|$.

Synthesis of the Salt $[NEt_4][closo$-1,2-Me_2-3-($\equiv CC_6H_4CH_2OMe$-2)-3,3-$(CO)_2$-3,1,2-$WC_2B_9H_9]$ (1d). A THF (20 mL) solution of $W(O_2CCF_3)(\equiv CC_6H_4CH_2OMe$-2)$(CO)_2(py)_2$[7] (1.64 g, 2.55 mmol) was treated with $Na_2[7,8$-$C_2B_9H_9Me_2]$ (2.70 mmol), the latter being obtained by refluxing $[NHMe_3][7,8$-$C_2B_9H_{10}Me_2]$[8] (0.60 g, 2.70 mmol) with an excess of NaH (0.55 g of a 60% dispersion in mineral oil, 13.8 mmol) in THF (10 mL). After the mixture was stirred for ca. 2 h, an excess of $[NEt_4]Cl$ (0.70 g, 3.80 mmol) was added, and the reactants were stirred for a further 30 min. The mixture was filtered through a Celite column (5 cm in length and 2 cm in diameter), and solvent was removed in vacuo. The residue was dissolved in CH_2Cl_2 (20 mL) and chromatographed at −20 °C. Elution with CH_2Cl_2–Et_2O (3:1) afforded an orange-red eluate. Solvent was removed in vacuo, and the oily residue was washed with Et_2O (3 × 20 mL) and dried in vacuo to give orange microcrystals of **1d** (1.50 g).

Protonations with $HBF_4{\cdot}Et_2O$. (i) A stream of CO was passed through a CH_2Cl_2 (20 mL) solution of **1d** (0.10 g, 0.15 mmol) at −78 °C for 5 min. The introduction of CO was continued while $HBF_4{\cdot}Et_2O$ (20 μL, 0.15 mmol) was added at −78 °C. The mixture was warmed slowly to room temperature. During this process the CO supply was maintained. After the mixture had been stirred for another 4–5 h, solvent was removed in vacuo. The residue was dissolved in CH_2Cl_2–hexane (10 mL, 1:1) and chromatographed at −30 °C. Elution with the same solvent mixture gave a light yellow eluate. Solvent was removed in vacuo to give green microcrystals of **6a** (0.045 g). This compound could also be

(7) Jeffery, J. C.; Li, S.; Stone, F. G. A. *J. Chem. Soc., Dalton Trans.* **1992**, 635.

(8) Hawthorne, M. F.; Young, D. C.; Garrett, P. M.; Owen, D. A.; Schwerin, S. G.; Tebbe, F. N.; Wegner, P. A. *J. Am. Chem. Soc.* **1968**, *90*, 862.

Table VII. Atomic Coordinates (×10⁴) and Equivalent Isotropic Displacement Parameters (Å² × 10³) for Complex 6b

atom	x	y	z	U(eq)[a]	atom	x	y	z	U(eq)[a]
W	11025 (1)	386 (1)	2356 (1)	28 (1)	C(36)	11145 (7)	2120 (3)	3993 (3)	40 (2)
P(1)	9678 (2)	157 (1)	1220 (1)	39 (1)	C(37)	12250 (7)	2445 (3)	3668 (3)	46 (2)
P(2)	10779 (2)	-136 (1)	3410 (1)	31 (1)	C(41)	8045 (7)	651 (3)	854 (3)	44 (2)
C(1)	13543 (6)	748 (3)	2716 (3)	37 (2)	C(42)	7169 (8)	430 (4)	274 (3)	61 (3)
C(2)	12960 (7)	925 (3)	1944 (3)	37 (2)	C(43)	5947 (8)	788 (4)	-13 (4)	72 (3)
C(3)	14504 (7)	134 (3)	2933 (3)	48 (2)	C(44)	5630 (8)	1374 (4)	265 (4)	68 (3)
C(4)	13394 (7)	490 (4)	1413 (3)	52 (2)	C(45)	6501 (7)	1604 (4)	845 (3)	57 (3)
B(3)	11409 (7)	1408 (3)	1830 (3)	35 (2)	C(46)	7714 (7)	1242 (3)	1138 (3)	51 (2)
B(4)	11045 (7)	1569 (3)	2631 (3)	31 (2)	C(51)	9128 (7)	-706 (3)	990 (3)	45 (2)
B(5)	12430 (7)	1092 (3)	3164 (3)	31 (2)	C(52)	8117 (8)	-1033 (4)	1258 (4)	64 (3)
B(6)	14471 (8)	1372 (4)	2377 (4)	43 (3)	C(53)	7700 (10)	-1676 (4)	1082 (4)	78 (4)
B(7)	13120 (8)	1781 (4)	1812 (4)	43 (3)	C(54)	8288 (11)	-2014 (4)	627 (5)	88 (4)
B(8)	11975 (8)	2173 (3)	2243 (4)	37 (2)	C(55)	9298 (10)	-1695 (4)	346 (4)	77 (4)
B(9)	12597 (7)	1978 (3)	3096 (3)	37 (2)	C(56)	9735 (8)	-1042 (4)	528 (3)	63 (3)
B(10)	14135 (7)	1466 (4)	3159 (4)	39 (2)	C(61)	12256 (6)	-572 (3)	3974 (3)	33 (2)
B(11)	13836 (8)	2139 (4)	2596 (4)	43 (2)	C(62)	12711 (7)	-1195 (3)	3823 (3)	44 (2)
C(20)	11595 (7)	-553 (3)	2216 (3)	39 (2)	C(63)	13768 (7)	-1543 (4)	4269 (3)	53 (3)
O(20)	12000 (6)	-1080 (2)	2122 (2)	59 (2)	C(64)	14393 (7)	-1261 (4)	4863 (3)	56 (3)
C(21)	8963 (6)	353 (3)	2368 (3)	39 (2)	C(65)	13931 (8)	-634 (4)	5015 (3)	59 (3)
O(21)	7764 (4)	368 (3)	2394 (2)	56 (2)	C(66)	12875 (7)	-285 (3)	4576 (3)	45 (2)
C(30)	9651 (6)	1876 (3)	2866 (3)	40 (2)	C(71)	9274 (6)	-707 (3)	3390 (3)	33 (2)
C(31)	9879 (6)	1845 (3)	3600 (3)	39 (2)	C(72)	9094 (7)	-1291 (3)	3012 (3)	53 (3)
C(32)	8895 (7)	1537 (3)	3903 (3)	51 (3)	C(73)	7929 (8)	-1705 (4)	3007 (4)	64 (3)
C(33)	9153 (8)	1495 (4)	4590 (4)	59 (3)	C(74)	6938 (8)	-1546 (4)	3369 (4)	64 (3)
C(34)	10391 (8)	1756 (4)	4971 (4)	60 (3)	C(75)	7106 (7)	-976 (4)	3745 (4)	59 (3)
C(35)	11383 (8)	2067 (3)	4677 (3)	53 (3)	C(76)	8274 (7)	-556 (3)	3761 (3)	47 (2)

[a] Equivalent isotropic U defined as one-third of the trace of the orthogonalized U_{ij} tensor.

Table VIII. Atomic Coordinates (×10⁴) and Equivalent Isotropic Displacement Parameters (Å² × 10³) for Complex 11

atom	x	y	z	U(eq)[a]	atom	x	y	z	U(eq)[a]
W(1)	1724 (1)	-1714 (1)	3179 (1)	43 (1)	W(2)	2624 (1)	3288 (1)	1797 (1)	44 (1)
I(1)	-1371 (2)	-1596 (1)	2951 (1)	72 (1)	I(2)	5618 (2)	3369 (1)	2095 (1)	80 (1)
C(121)	1043 (22)	-266 (16)	3273 (6)	48 (7)	C(221)	3330 (26)	4767 (19)	1699 (7)	63 (9)
O(121)	711 (22)	635 (14)	3372 (6)	88 (8)	O(221)	3665 (20)	5633 (12)	1617 (5)	76 (7)
C(122)	3547 (28)	-857 (21)	2933 (8)	75 (10)	C(222)	783 (28)	4160 (18)	2003 (8)	67 (9)
O(122)	4543 (20)	-338 (15)	2820 (7)	107 (9)	O(222)	-259 (19)	4709 (14)	2104 (6)	91 (8)
C(123)	1844 (27)	-1935 (17)	2498 (10)	75 (10)	C(223)	2202 (26)	3077 (17)	2513 (9)	65 (9)
O(123)	2213 (24)	-2087 (13)	2074 (5)	96 (8)	O(223)	2098 (23)	2866 (13)	2882 (5)	91 (8)
C(101)	2476 (23)	-3553 (14)	3290 (7)	52 (7)	C(201)	1913 (30)	1484 (14)	1667 (7)	65 (9)
C(102)	2695 (27)	-4138 (18)	2830 (8)	76 (10)	C(202)	1536 (26)	845 (17)	2126 (7)	73 (9)
B(102)	3807 (25)	-2631 (21)	3412 (9)	59 (9)	B(202)	612 (32)	2379 (20)	1517 (10)	67 (11)
B(103)	2882 (26)	-1710 (16)	3853 (8)	43 (8)	B(203)	1660 (26)	3312 (18)	1086 (8)	48 (8)
B(104)	893 (24)	-2143 (15)	3989 (7)	36 (7)	B(204)	3690 (25)	2901 (16)	1010 (7)	41 (7)
B(105)	717 (25)	-3255 (16)	3601 (7)	42 (7)	B(205)	3693 (27)	1710 (18)	1425 (8)	49 (8)
B(106)	3721 (34)	-3958 (22)	3649 (10)	71 (11)	B(206)	718 (34)	1098 (20)	1289 (11)	72 (11)
C(107)	3853 (24)	-2889 (16)	4001 (7)	56 (8)	C(207)	717 (21)	2215 (15)	921 (7)	46 (7)
C(108)	5436 (21)	-2671 (19)	4152 (7)	68 (9)	C(208)	-704 (22)	2445 (18)	686 (8)	71 (9)
B(108)	2210 (27)	-2525 (18)	4366 (8)	51 (8)	B(208)	2480 (25)	2477 (16)	580 (8)	44 (8)
B(109)	790 (23)	-3456 (16)	4220 (7)	40 (7)	B(209)	3764 (23)	1554 (15)	787 (7)	36 (7)
B(110)	1760 (32)	-4325 (20)	3788 (8)	60 (9)	B(210)	2721 (27)	665 (15)	1201 (7)	46 (8)
B(111)	2747 (30)	-3902 (19)	4245 (9)	58 (9)	B(211)	1938 (29)	1099 (18)	694 (10)	59 (9)
C(130)	-579 (20)	-1491 (14)	4265 (6)	43 (6)	C(230)	5252 (24)	3461 (14)	759 (6)	51 (7)
C(131)	-1033 (21)	-1778 (15)	4785 (6)	44 (7)	C(231)	5881 (20)	3178 (15)	265 (6)	42 (7)
C(132)	-1451 (21)	-1010 (18)	5135 (7)	58 (8)	C(232)	6416 (23)	3927 (17)	-70 (8)	59 (8)
C(133)	-1737 (25)	-1283 (20)	5607 (7)	65 (9)	C(233)	6947 (24)	3677 (19)	-533 (8)	65 (9)
C(134)	-1714 (23)	-2283 (20)	5763 (8)	62 (9)	C(234)	6972 (23)	2660 (20)	-684 (7)	64 (9)
C(135)	-1402 (22)	-3055 (18)	5427 (7)	58 (8)	C(235)	6443 (22)	1849 (19)	-348 (7)	60 (8)
C(136)	-1044 (21)	-2834 (15)	4930 (6)	43 (6)	C(236)	5912 (21)	2121 (16)	125 (6)	46 (7)
C(137)	-672 (25)	-3701 (14)	4580 (7)	60 (8)	C(237)	5383 (25)	1261 (15)	467 (8)	63 (8)
N(1)	6891 (19)	2564 (15)	3771 (6)	62 (7)	N(2)	7653 (19)	-2457 (14)	1291 (6)	58 (7)
C(141)	7393 (28)	1674 (22)	4074 (9)	83 (11)	C(241)	8194 (29)	-2884 (21)	1725 (8)	83 (11)
C(142)	6182 (39)	916 (27)	4279 (13)	153 (20)	C(242)	6942 (28)	-3421 (22)	2059 (9)	100 (12)
C(143)	6207 (28)	2168 (20)	3366 (9)	86 (12)	C(243)	7198 (28)	-3338 (20)	993 (9)	84 (11)
C(144)	7354 (27)	1556 (17)	2980 (9)	83 (10)	C(244)	8453 (32)	-4170 (22)	823 (10)	119 (15)
C(145)	5583 (26)	3229 (23)	4081 (9)	86 (11)	C(245)	6287 (30)	-1724 (25)	1395 (10)	99 (13)
C(146)	6121 (38)	3780 (28)	4471 (10)	159 (20)	C(246)	6429 (39)	-792 (23)	1703 (11)	133 (17)
C(147)	8281 (27)	3220 (22)	3614 (9)	83 (11)	C(247)	9004 (29)	-1853 (22)	1056 (8)	85 (11)
C(148)	8075 (32)	4112 (22)	3293 (11)	114 (15)	C(248)	8725 (40)	-1285 (26)	616 (10)	126 (17)

[a] Equivalent isotropic U defined as one-third of the trace of the orthogonalized U_{ij} tensor.

prepared in the absence of CO, but the yield was lower (0.032 g, 36% yield).

(ii) A CH_2Cl_2 (20 mL) solution of **1d** (0.10 g, 0.15 mmol) and PPh_3 (0.090 g, 0.34 mmol) was treated with $HBF_4 \cdot Et_2O$ (20 μL, 0.15 mmol) at −78 °C. The mixture was then warmed slowly to room temperature. The mixture was stirred for 4 h at room temperature, after which solvent was removed in vacuo. The residue was dissolved in CH_2Cl_2–hexane (10 mL, 1:1) and chro-

matographed. Elution with the same solvent mixture afforded a yellow eluate. Solvent was removed in vacuo, and the residue was crystallized from CH_2Cl_2–hexane (10 mL, 1:4) to give yellow microcrystals of **7a** (0.076 g), after washing with hexane (2 × 5 mL) and drying in vacuo.

(iii) Using a similar procedure, a CH_2Cl_2 (20 mL) solution of **1d** (0.10 g, 0.15 mmol) mixed with a solution of PPh_2H in CH_2Cl_2 (0.13 M, 2.0 mL, 0.26 mmol) was treated with $HBF_4{\cdot}Et_2O$ (20 μL, 0.15 mmol) at −78 °C to give yellow microcrystals of **6b** (0.089 g).

(iv) In a similar synthesis, a solution of **1d** (0.10 g, 0.15 mmol) and $Ph_2PCH_2PPh_2$ (0.065 g, 0.17 mmol) in CH_2Cl_2 (20 mL) was treated with $HBF_4{\cdot}Et_2O$ (20 μL, 0.15 mmol) at −78 °C to afford yellow microcrystals of **8** (0.095 g).

(v) Similarly, a CH_2Cl_2 (20 mL) solution of **1d** (0.10 g, 0.15 mmol) was treated with $HBF_4{\cdot}Et_2O$ (20 μL, 0.15 mmol) at −78 °C in the presence of PhC≡CPh (0.060 g, 0.34 mmol) to yield yellow microcrystals of **9** (0.073 g).

Protonation with HI. A CH_2Cl_2 (20 mL) solution of **1d** (0.10 g, 0.15 mmol) was treated with 57% aqueous HI (100 μL, 0.70 mmol) at room temperature. After the mixture was stirred for 4 h, solvent was removed in vacuo. The residue was dissolved in CH_2Cl_2 (10 mL) and chromatographed on a short alumina column (2 × 4 cm) at −30 °C. Elution with CH_2Cl_2–Et_2O (3:1) gave a brown eluate. Solvent was removed in vacuo, and the residue was crystallized from CH_2Cl_2–hexane (5 mL, 1:4) to give dark red microcrystals of **11** (0.057 g).

Reaction of the Salt 11 with $Bu^tC{\equiv}CH$. A sample of the salt **1d** (0.40 g, 0.60 mmol) was treated with aqueous HI to obtain **11**, as described above. The latter was dissolved in CH_2Cl_2 (20 mL) and treated with $Bu^tC{\equiv}CH$ (100 μL, 0.81 mmol), followed by an excess of $TlBF_4$ (ca. 0.50 g, 1.72 mmol). The mixture was then stirred for 4 h. Solvent was removed in vacuo, and the residue was dissolved in CH_2Cl_2–hexane (10 mL, 1:1). Chromatography, with the same solvent mixture as eluent, gave a purple fraction. Solvent was removed in vacuo, and the residue was extracted with hexane (10 mL). The remaining white solid was dried in vacuo to give pale yellow microcrystals of **13** (0.152 g). The hexane extracts were rechromatographed to yield purple microcrystals of **12** (0.034 g).

Crystal Structure Determinations. The crystal data and other experimental details for the compounds **6b** and **11** are given in Table VI. Crystals of **6b** were grown from CH_2Cl_2–hexane (1:5) as yellow prisms and those of **11** similarly as orange cubes. Crystal dimensions were ca. 0.30 × 0.50 × 0.20 mm (**6b**) and ca. 0.40 × 0.45 × 0.30 mm (**11**). The data were corrected for Lorentz, polarization, and X-ray absorption effects, the last by a method based on azimuthal scan data.[9] The structures were solved by conventional heavy-atom and difference Fourier methods, by which all non-hydrogen atoms were located and refined anisotropically. Terminal B–H hydrogens were included in the refinement of **6b**, but not of **11**; all remaining hydrogens were included in calculated positions (C–H = 0.96 Å) with fixed isotropic thermal parameters (U_{iso} = 0.08 Å^2).

Calculations were performed on a Digital micro-Vax II computer with the SHELXTL PLUS system of programs.[9] Scattering factors with corrections for anomalous dispersion are included in the program. Atomic coordinates for **6b** and **11** are given in Tables VII and VIII.

Acknowledgment. We thank the British Council and the State Education Commission of the People's Republic of China for a studentship (to S.L.) under the Sino-British Friendship Scholarship Scheme and the Robert A. Welch Foundation for support (S.L. and F.G.A.S.).

Supplementary Material Available: Complete tables of bond lengths and bond angles, anisotropic thermal parameters, and hydrogen atom parameters for **6b** and **11** (17 pages). Ordering information is given on any current masthead page.

OM910696S

(9) SHELXTL PLUS programs for use with the Siemens R3m/V X-ray system, by G. M. Sheldrick.